Tuning surface grafting density of CeO2 nanocrystals with near- and supercritical solvent characteristics.

Baptiste Giroire, Cédric Slostowski, Samuel Marre, Cyril Aymonier, Tsutomu Aida, Daisuke Hojo, Nobuaki Aoki, Seiichi Takami, Tadafumi Adschiri

PCCP

Paper

Tuning surface grafting density of CeO_2 nanocrystals with near- and supercritical solvent characteristics

Received 00th January 20xx,
Accepted 00th January 20xx

DOI: 10.1039/x0xx00000x

www.rsc.org/

B. Giroire[a,b], C. Slostowski[a,b], S. Marre[a,b] and C. Aymonier*[a,b]

T. Aida[c], D. Hojo[c], N. Aoki[c], S. Takami[c] and T. Adschiri*[c]

In this work, the solvent effect on the synthesis of CeO_2 nanocrystals prepared in near- to supercritical alcohols is discussed. The material prepared displayed a unique morphology of small nanocrystals (< 10 nm) agregated into larger nanospheres (~100 – 200 nm). In such syntheses, alcohol molecules directly interact with the nanocrystal surface through alkoxide and carboxylate bondings. The grafting density was quantified from the weight loss measured using thermogravimetric analysis. A direct correlation between the grafting density and the alcohol chain length can be established. It was demonstrated that the shorter the alcohol chain length (*i.e.* Methanol), the higher the surface coverage is. This trend is independent of the synthesis mode (batch or continuous). Additionaly, an influence of the grafting density on the resulting nanocrystal size was established. It is suggested that the surface coverage has a high influence on the early stages of the nucleation and growth. Indeed, when high surface coverages are reached, all surface active sites are blocked, limiting the growth step and therefore leading to smaller particles. This effect was noticed with the materials prepared in continuous where shorter reaction time were performed.

Introduction

Over the past 30 years, synthesis of cerium oxide (CeO_2) bulk and nanoparticles has been widely studied for various applications such as catalysis;[1,2,3] polishing materials[4,5,6] and UV blocker.[7,8,9] A control of the nanocrystals (NCs) formation steps is key to improve homogeneity in physical properties and therefore, to produce high quality materials. In this regard, hydrothermal syntheses have been extensively studied, and especially at supercritical conditions, where the fluid (water, alcohols, mixtures, etc) properties can be tuned with pressure and temperature[10,11,12,13] allowing a control of the NCs nucleation and growth. The first report on cerium oxide synthesis at supercritical conditions was performed in water by Adschiri et al.,[14,15] similarly to their previous works dealing with other metal oxides syntheses. Close to its critical point (T_c = 374 °C, p_c = 22.1 MPa), the dielectric constant of water greatly decreases, resulting in faster nucleation of metal oxides nanocrystals due to the high supersaturation of the metal ions in solution,[16] with a possibility to access a fine control of the material composition.[17,18] Moreover, due to its low dielectric constant, near- or supercritical (nc- or sc-) water acts as an organic solvent, leading to high miscibility with organic molecules. Therefore, hybrid organic/inorganic cerium oxide nanoparticle synthesis can be achieved in one step in a continuous reactor.[19] The size and morphology of nanoparticles are then controlled by the interaction between the organic surfactant and the growing CeO_2 NCs.[20]

The formation of such hybrid organic/inorganic nanomaterials prevents particle aggregation and allows the production of colloidal solution,[21] ideal for a better processability of the nanoparticles. They also allow the use of cerium oxide for healthcare applications, such as skin protection against organophosphates[22] or targeted delivery of the CeO_2 with an antioxidant action.[23]

Common surface modifiers such as carboxylic acids, fatty acids (*e.g.* oleic acid), and amine (*e.g.* oleylamine) have been used for the functionalization of cerium oxide nanoparticles (NPs).[24,25,26,27] Carboxylic groups preferably bind to the {100} surface through bidentate chelate, chelate bridging or unidentate interactions, leading to the formation of nanocubes.[24,28] Cerium oxide with truncated octahedron morphology can be obtained with {111}, {020} and {220} (edges) exposed with excess in surfactant. However, most common fatty acids are little soluble in water at room temperature, which generates issues for continuous syntheses. Thus, most of the metal oxide functionalization studies in water have been performed in batch reactor where the organic modifier becomes soluble when supercritical conditions are reached.[19,29]

[a] CNRS, ICMCB, UPR 9048, F-33600 Pessac, France
Email: cyril.aymonier@icmcb.cnrs.fr
[b] Univ. Bordeaux, ICMCB, UPR 9048, F-33600 Pessac, France
[c] WPI-Advanced Institute for Material Research, Tohoku University
Email: ajiri@tagen.tohoku.ac.jp
† Footnotes relating to the title and/or authors should appear here.
Electronic Supplementary Information (ESI) available: See
DOI: 10.1039/x0xx00000x

In a previous study, it was shown that the alkyl chain length of carboxylic acid (from C6 to C18) has an influence on the resulting surface coverage of CeO_2 synthesized in water.[30] High surface coverage, up to 6.7 molecules.nm^{-2} (corresponding to a surface coverage of 98 %), were recorded for the longest alkyl chain length (C18). A gradual increase in the surface coverage with increasing alkyl chain length was observed and explained by an increase in the hydrophobic interactions between alkyl chains.

More recently, Veriansyah et al. investigated for the first time the use of an alcohol, i.e. methanol.[31,32] They proposed, that methanol could interact with the particle surface through methylate, methoxide and hydroxide bonds. Following their work, our previous study broadened this investigation to the 6 first primary alcohols (from methanol to hexanol) and isopropanol, in near- or supercritical conditions. It was demonstrated that near- and supercritical alcohols act not only as solvents for the synthesis but also as surface modification agents of the cerium oxide through the formation of alkoxide and carboxylate bounds.[33] The use of alcohols as solvents and surface modification agents of CeO_2 NCs presents the advantage to be compatible with continuous system. Furthermore, a direct correlation between the alcohol chain length and the resulting CeO_2 NCs size was established. The obtained NCs (3-7 nm depending on the alcohol) were found to be aggregated into bigger nanospheres. These newfound properties of near- and supercritical alcohols were later implemented in order to synthesize CeO_2 NCs (i) with finely controlled crystallite sizes using alcohols mixtures and (ii) with chosen surface functionalities using alcohol derivatives (e.g., aminoalcohols for CeO_2 NCs with $–NH_2$ surface functionalization).[34] Finally, after a thermal treatment at 500 °C, CeO_2 NCs synthesized in near- and supercritical alcohols displayed record specific surface area (up to 200 g.cm^{-2}), suggesting further interest for investigating the materials catalytic properties, for example.[35] Regarding the aforementioned information on the influence of the alcohol nature on the cerium oxide crystallite size, the grafting density seems to be one of the key issue to better understand and control the growth mechanism of these materials.

With this in mind, the present work proposes a quantification of the grafting density of alcohols attached to the surface of the cerium oxide NCs produced in near- or supercritical alcohols. Synthesis of CeO_2 NCs in alcohols was conducted in batch mode since most reports of surface modification of cerium oxide were performed in batch reactors. A comparison between materials synthesized in batch and in continuous reactions is proposed to better understand the evolution of CeO_2 NCs size as a function of the alcohol chain length based on thermogravimetric analyses.

Experimental

Materials and methods.

Methanol (MeOH, purity ≥ 99.9%), ethanol (EtOH, purity ≥ 99.8%), butan-1-ol (ButOH, purity ≥ 99.9%), hexan-1-ol (HexOH, purity 98%), propan-2-ol (isopropanol, iPrOH, purity ≥ 99.5%), and cerium (III) nitrate hexahydrate (purity ≥ 99,0 %) were purchased from Sigma Aldrich and used as received. All chemicals were used as received with no further purification.

Batch reactor synthesis. Cerium nitrate hexahydrate (143 mg) was dissolved in 2.62 mL of the corresponding alcohol ([Ce^{3+}] = 10^{-1} M) in a Hastelloy C batch reactor having a total volume of 5 mL. The temperature of the reaction was set at 300 °C. In such conditions, reactions in methanol, ethanol and isopropanol were performed at supercritical conditions, whereas the reactions in butanol and hexanol were performed at near-critical conditions. The small batch reactor was inserted in a preheated furnace to ensure a fast heating of the sample[36]. The furnace was rocked during the reaction to improve the mixing inside the reactor, hence, the homogeneity of the reaction media. After 10 minutes of reaction, the batch reactor was removed from the hot furnace and plunged into an iced-water tank to quench the reaction. All samples were washed three times through centrifugation steps with the corresponding alcohols. Particle and crystallite sizes (d_{TEM} and d_{XRD}, respectively) of the resulting powders are reported in Table 1.

Looking at the temperature profile of the batch reactor (see supporting information, Figure S1), it was assumed that the nucleation steps occurred in near-critical conditions for all alcohols, since the critical temperature was only reached two to three minutes after starting the heating of the sample. Thus the main focus of this study concerns the characterization of the materials, in order to quantify the grafting density of alcohol-modified CeO_2 NCs and therefore to have a better understanding of the formation mechanism, TGA experiments were particularly used.

As a matter of comparison with batch synthesis, cerium oxide nanocrystals synthesized continuously in near- and supercritical alcohols are evoked in this manuscript. Their synthesis method and conditions have been described in our previous work, along with their characteristics.[33]

Characterization.

The XRD patterns were recorded on a Rigaku SmartLab 9MTP. The TEM images were acquired using a Hitachi H-7650 with an acceleration voltage of 100 kV. Samples were prepared by direct deposition of particles dispersed in ethanol on copper-carbon grids. The FTIR measurements were obtained using a JASCO FT/IR-4200. The spectra were recorded over 32 scans in the range of 400-4000 cm^{-1}. Samples were prepared by mixing cerium oxide powder with KBr and pressed into pellets. Thermo Gravimetric Analyses (TGA) were performed from room temperature up to 800 °C with a heating rate of 2 °C.min^{-1} under a nitrogen atmosphere using a TG-DTA Shimadzu DTG-60AH. Measurements were made on powder samples of approximately 10 mg.

Grafting density calculation. The amount of surface modifier attached to the particle surface was estimated from the TGA results. These calculations were made considering spherical particles, a density of CeO_2 NCs of 7.172 g.cm^{-3} [7], a homogeneous size distribution and a uniform coverage at the surface of each particle with the organic modifier. The grafting density (molecule.nm^{-2}) was estimated using the three following equations:

$$N_{NP} \times \left(\frac{4\pi r^3}{3}\right) = \left(\frac{m_0 \times \frac{100-a}{100}}{\rho_{CeO_2}}\right) \quad \text{Eq. 1}$$

$$S = N_{NP} \times 4\pi r^2 \quad \text{Eq. 2}$$

$$N_f = \left(m_0 \times \frac{a}{100}\right) / M_f \times N_A \quad \text{Eq. 3}$$

Where r, N_f and N_{NP} are the radius (nm), the total number of organic functions attached to the nanoparticles (number) and the total number of nanoparticles in the studied sample (number), respectively; m_0, a, and ρ_{CeO2} are the starting mass (g), the product's weight loss (%) and the density of bulk cerium oxide (7.172 g.cm^{-3}), respectively ; S, M_f and N_A are the total surface area of the nanoparticles (nm^2), the molecular weight of the organic ligand (g.mol^{-1}) and the Avogadro number (6.02 x 10^{23}), respectively. The grafting density was then calculated by dividing equation 3 by equation 2. Calculations were made using the size of the particles measured with TEM.

Results and discussion

XRD patterns of the as-prepared particles (without annealing step) are shown in Figure 1.

Cerium oxide synthesized in alcohol possesses a fluorite structure ($Fm\bar{3}m$ space group). All experiments showed the synthesis of well crystallized cerium oxide nanoparticles having a lattice parameter of 5.41 ± 0.01 Å. The crystallite sizes (d_{XRD}) of the nanoparticles were determined using Scherrer's equation (Table 1).

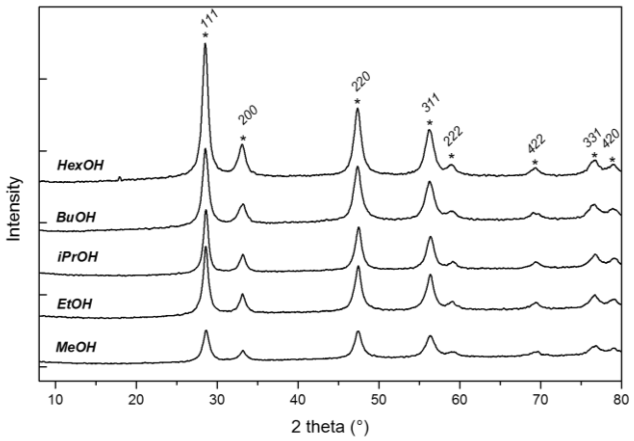

Figure 1 XRD patterns of the CeO_2 powders recovered from batch synthesis in scMeOH, scEtOH, scButOH and ncHexOH (300 °C; 10 min). (*Peaks have been indexed from the JCPDS file n°34-0394, corresponding to cerianite - CeO_2

Table 1 Particle (d_{TEM}) and crystallite (d_{XRD}) sizes of the CeO_2 nanopowders synthesized in near- or supercritical (nc- and sc-) alcohols in batch reactor (300 °C, t_r = 10 min).

Solvent name	Reaction Conditions	d_{TEM} (nm)[a]	d_{XRD} (nm)[b]
Methanol	sc	5.0 ± 0.5	7.2 ± 0.5
Ethanol	sc	5.4 ± 0.5	7.9 ± 0.5
Butanol	nc	5.8 ± 0.6	7.4 ± 0.6
Hexanol	nc	5.0 ± 0.5	7.7 ± 0.6
Isopropanol	sc	6.0 ± 0.6	8.9 ± 0.7

[a]*Particle sizes (d_{TEM}) have been analyzed using the ImageJ software by counting over 100 particles.*
[b]*Crystallite sizes (d_{XRD}) are calculated from the X-ray patterns using the Scherrer equation (higher intensity diffraction peak (111)).*

The morphology of the CeO_2 nanopowders synthesized in alcohol was investigated by Transmission Electron Microscopy (TEM). Representative pictures are shown in Figure 2. Similarly to the powders obtained in continuous flow in our previous work,[33] the CeO_2 nanopowders prepared in batch reactor displayed a unique morphology: big spherical shapes, with sizes ranging from 100 to 700 nm, which are composed of smaller aggregated nanoparticles. This kind of morphology suggests the functionalization of the CeO_2 nanoparticles with nonpolar groups.[33] No significant differences in the morphology of the powders were observed among the different samples, although the cerium oxide synthesized in hexanol seemed to have wider sphere size dispersion. The average sizes of the nanoparticles measured by image analysis (d_{TEM}) are given in Table 1. Although there are differences

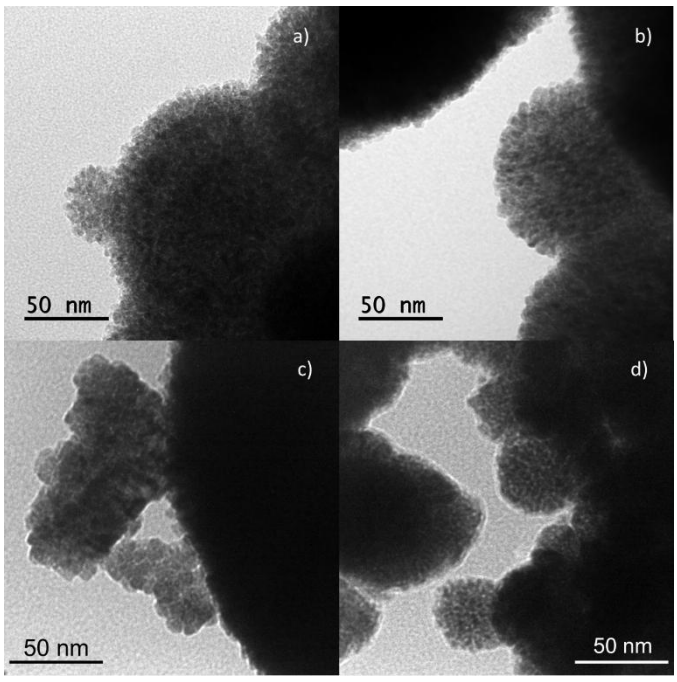

Figure 2 TEM pictures of CeO_2 synthesized in batch reactor at 300 °C (Rt = 10 min) in (a) sc-methanol, (b)

between the size of the nanoparticles measured by TEM and by XRD, the trend is the same for all alcohols. Similar sizes of approximately 5-6 nm were obtained for all samples. Alcohol chain length did not impact the particle size as much as in the continuous experiments.[33] This altered behavior can be explained by the differences in heating rates (see Figure S1) in the two systems as well as a different oxidation state of the cerium atom in the precursor used, leading to changes in the nucleation and growth rates. Indeed, after one minute, the reaction is done and quenched for the continuous system whereas the batch reactor only reached approximately 200 °C. Additionnaly, longer reactions times were performed in batch conditions, favoring growth.[37] The unique morphology observed in these syntheses can be explained as follow: (i) after nucleation, particles are growing from nuclei, then the growth of the particles is stopped by the grafting of alcohols molecules, (ii) the particles being quite small (less than 8 nm), and carbon chain length below C6, surface energies are important and thus, the particles tend to aggregate in larger round shapes in order to reduce the total surface energy and (iii) after grafting, the cerium oxide surface becomes hydrophobic, which does not favor dispersion into alcohols.

The surface of the as-prepared CeO_2 NCs was characterized using FTIR spectroscopy in order to study the organic surface properties of CeO_2 NCs synthesized in batch mode. Indeed, we demonstrated in our previous work that nc- and sc-alcohols act as solvent and surface modification agent of the CeO_2 during the synthesis in continuous flow, leading to the formation of alkoxides and carboxylates on CeO_2 NCs surface.[33,34] Spectra of the CeO_2 NCs synthesized in batch in nc- and sc-alcohols are shown in Figure 3.

Firstly, all samples present a broad band centered at approximately 490 cm^{-1}, being the signature of a Ce-O bond in the CeO_2 crystal,[38] which is consistent with the results obtained by XRD. Moreover, a broad hydroxyl stretching vibration band (–OH) is observed at 3750-3000 cm^{-1} (Figure 3.a – Area A). These surface hydroxides cannot only be attributed to the interaction of water (from the atmosphere or the solvent) with CeO_2 NCs but also to the grafting of alcohols on the surface of the materials leading to the formation of alkoxides and carboxylates via the dehydration of the alcohols.[33,39,40]

Weak bands corresponding to the symmetric and asymmetric stretching vibrations of methylene ($–CH_2–$) and methyl ($–CH_3$) are observed in the 3000-2800 cm^{-1} region (Figure 3.a - Area B). The intensity of these bands, becoming stronger when the carbon chain of the alcohol used as solvent is increasing (ButOH and HexOH), supports the presence of alcohols on the surface of CeO_2 NCs synthesized in batch. Furthermore, the presence of stretching vibration bands is attributed to carboxylate (–COO) and alkoxide (–C–O) groups, visualized respectively in the areas C and D in Figure 3.a. These interaction types confirm that organic species detected at the surface of the CeO_2 NCs correspond to grafted alcohols and not to solvent residues. These two latter areas of Figure 3.a give information about the interaction types formed between

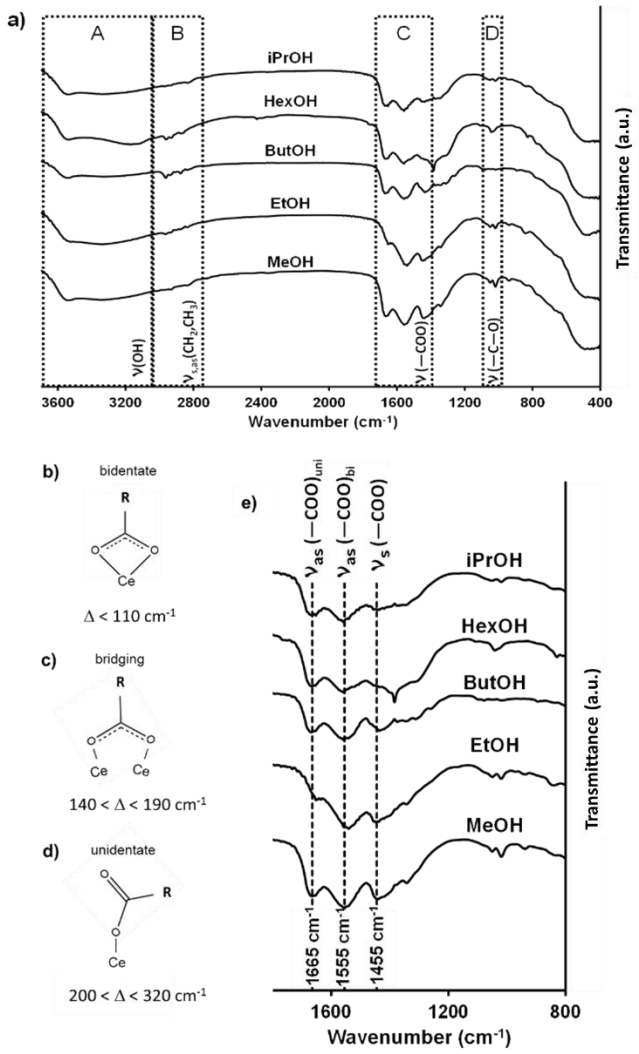

Figure 1 (a) IR spectra of the surface modified CeO_2 powders obtained during the synthesis in nc- and sc-alcohols in batch at 300 °C (t_r = 10 min) and (e) enlargement in the 1800-800 cm^{-1} region. Representation of (b) bidentate chelate, (c) chelate CeO_2 NCs and alcohols during the synthesis in nc- and sc-alcohols. The very weak band observed around 1050 cm^{-1} corresponding to the stretching vibration band of the alkoxide (characteristics of alcohols moiety), has been attributed to the grafting of an alcohol molecule at the CeO_2 surface through the formation of an alkoxide bond and the dehydration of the alcohols (formation of surface O–H bond). The weakness of this band compared to the higher intensity bands in the carboxylate region around 1700-1400 cm^{-1} (area C) may be due to a smaller proportion of alkoxide interaction type compared to the carboxylate interaction type. The carboxylate interaction of the alcohol with the CeO_2 NCs is characterized through its symmetric and asymmetric vibration bands in the 1700-1400 cm^{-1} region, as shown in the area C of the Figure 3.a. The formation of such interaction type is driven by a second dehydration of the grafted alcohol (leading to the formation of another surface O–H bond) and the interaction between the dehydrated carbon of this alkoxide and a surface

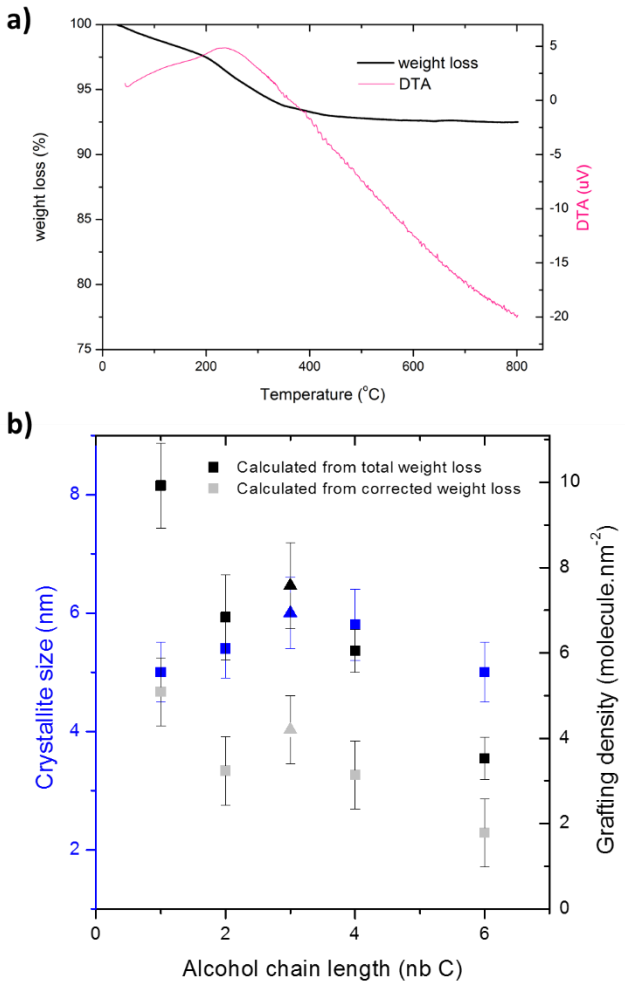

Figure 4 (a) Typical TGA and DTA curves of CeO_2 NPs prepared in nc- or sc-alcohols (here ethanol) (b) crystallite size and grafting density of CeO_2 NCs

oxygen atom of the CeO_2 NCs. This interaction could lead to the formation of three different types of carboxylates, as depicted by Taguchi *et al.*[27]: chelating bidentate, bridging or unidentate carboxylates. The difference (Δ) in wavenumber between the symmetric and the asymmetric stretching vibration bands of the carboxylate group allows determining the type of carboxylate involved, as described in Figure 3.b, c and d.

Figure 3.e shows an enlargement of the 1800-800 cm^{-1} region for each IR spectrum, in order to better determine the types of carboxylate interaction formed on the surface of CeO_2 NCs during the batch synthesis in nc- and sc- alcohols. A previous work allowed us to identify the formation of chelating bidentate type interaction ($\Delta < 110$ cm^{-1}) during the synthesis in continuous flow in nc- and sc-alcohols.[34] The same interaction is also found inhere for the CeO_2 NCs synthesized in batch, with a symmetric vibration band around 1455 cm^{-1} and an asymmetric one around 1555 cm^{-1} (Δ around 100 cm^{-1}).

Furthermore, another band is detected around 1665 cm^{-1}. This band can also be attributed to an asymmetric vibration band of the carboxylate interaction but of the unidentate type (210 $cm^{-1} < \Delta < 320$ cm^{-1}).

Therefore, IR spectra of the CeO_2 NCs allow identifying the formation of three different types of interaction between the surface of the oxide and the alcohol during the batch synthesis: (i) alkoxide, (ii) chelating bidentate and (iii) unidentate interaction types. As a comparison, CeO_2 NCs synthesized in continuous flow displayed only the alkoxide and chelating bidentate interaction types after the synthesis in nc- and sc-alcohols, and the intensity of the alkoxide band was stronger,[33,34] indicating a stronger grafting of molecules to the particle surface since the unidentate interaction type (present only in CeO_2 prepared in batch) is the weakest of the three types of interaction.

Note that the band intensities correlate with the number of chemisorbed functions attached to the nanoparticles surface.[30] The intensities of the contributions attributed to the surface modifiers appear to gradually increase with shorter alcohol chain length, as seen in Figure 3e, indicating a higher grafting density. A broadening of the symmetric stretching vibrations of the –COO group (centered at 1455 cm^{-1}) is also observed when decreasing the alcohol chain length. This observation is due to an increase of the intermolecular interactions, in agreement with dense modification of the particle surface. The same observation can be made when comparing NCs prepared in primary alcohols and secondary alcohols (isopropanol): a broader feature is observed for primary alcohols, suggesting a higher surface coverage for primary alcohols.

Indeed, the formation of the alkoxide is the first to happen. This step can either be followed by the desorption of the alcohol or the formation of the chelating bidentate, more stable than the alkoxide, via the dehydration of the alkoxide[33]. These phenomena can be favored with time and temperature, explaining the difference of intensity between batch mode and continuous flow synthesis. But, as described by Idriss *et al.*,[39,40] the carboxylate can be broken over time and temperature resulting in various byproducts such as ketones, aldehydes, alkyl acetate, etc. Thus, the presence of the unidentate interaction types on the CeO_2 NCs synthesized in batch could be a transitional state towards the desorption of the chelating bidentate type carboxylate with temperature and time. This behavior was not observed previously in the sample prepared in continuous due to shorter reaction times.

Weight losses of the samples prepared in batch are presented in Figure 4a. A small weight loss (< 4 wt.%) is observed between room temperature and 175 °C, arising from small molecules adsorbed to the surface or alcohols molecules attached through alkoxide bond. Reports from the literature and DTA curves showed that temperatures above 200 °C are required to start breaking the carboxylate bonds between the surface modifier and the cerium atoms at the surface of the CeO_2 nanoparticles.[30] Most of the weight loss of our samples occurs in the 200 - 400 °C range, in agreement with carboxylic acid removal.

Due to the relative small size of the surface modifier, physical absorption of water or CO_2 molecules is possible at room temperature. Therefore, corrections on the total weight loss measured from the TGA experiments were applied to determine more accurate values on the surface coverage of nanoparticles (see below). The calculations of surface coverage were performed using the particle size measured by TEM.

The quantity of undesired light molecules adsorbed to the surface of the sample prepared in batch conditions was estimated by an indirect method. All organic modifiers were removed from the sample after a thermal treatment at 800 °C.[27,30] The powder was then let under air for 48 hours. TGA analyses were performed on these samples and the weight loss was attributed to a maximum value of CO_2 and water attached to the particle surface. This value was removed from the total weight loss. Although, this calculation does not yield an exact value of the surface coverage, the theoretical lower (corrected weight loss) and higher (total loss) surface coverage are presented in Figure 4b. The actual grafting density values are between these lower and upper limits; and as of today it would be difficult to obtain more accurate values. A gradual decrease in surface coverage was measured for the sample prepared in batch, as seen in Table 2. Such decrease was expected from the analysis of the shape (width and relative intensity) of the IR spectra. Direct comparison between grafting densities is possible since particles have similar sizes (all within the same error bar for primary alcohols). Therefore, an assessment on the interaction of the alcohol molecules with the CeO_2 surface can be made. High/fast kinetics of alcohol grafting is probable for short primary alcohols. An increase of the steric hindrance (due to free rotation) with increasing alcohol chain length could lead to a decrease in surface coverage. Note that the theoretical surface coverage of CeO_2 with fcc structure and a lattice constant of 5.4112 Å was estimated to be 6.84 molecules.nm^{-2}, which corresponds to the number of cerium ions available on the surface of the {100} plane CeO_2 NCs.[26] The {100} surface is considered to be the most reactive and therefore the organic/inorganic interaction are favored at this interface.[30] Correlation of surface coverage and particle size with alcohol chain length is presented in Figure 4b.

As a matter of comparison with the results obtained in batch mode and to better apprehend the influence of alcohol grafting during the cerium oxide synthesis, result obtained from the synthesis of CeO_2 NCs from ammonium cerium (IV) nitrate in continuous flow are shown in Figure S2. The detailed process description and characterization of the NCs prepared is available elsewhere.[33] A direct relationship between the alcohol chain length and the particle size could be established for the material produced in continuous. Here, a direct relationship between the surface coverage and the particle size can be observed. It was concluded that the smaller the nanoparticles, the higher the surface coverage is, as seen in Figure S2b. Due to the small steric hindrance of the methanol molecule, a high surface coverage of the cerium oxide is expected during the nanoparticle formation. Therefore, active surface states of nanoparticles are readily blocked and the nanoparticle growth is quenched. A lower surface coverage is anticipated for longer alcohol i.e. hexanol, due to higher steric hindrance induced by free rotation of the longer carbon chain. Active surface states are therefore more accessible to the precursor during the reaction and growth of CeO_2 nanoparticles is possible resulting in larger nanoparticles. The continuous increase of the nanoparticle size is consistent with the increase of the steric hindrance, with increasing alcohol chain length.

Similar influence of alcohol chain length on the surface coverage was observed for the CeO_2 NCs obtained in batch, even if no effect on the particle morphology could be extracted from these samples. Increased reaction times, slower heating rates (see Figure S1) as well as differences in formation mechanism (different oxidation state of cerium precursors) can explain this change in behavior.

CeO_2 NCs prepared in secondary alcohol (isopropanol) displayed bigger crystallite sizes. However, the grafting densities measured in both batch and continuous were slightly higher than samples prepared in the corresponding primary alcohol (propanol). This difference can be explained in differences in grafting kinetics. Knowing that the grafting of the secondary alcohol to the surface happens through an alkoxide bond in the early stage of the material formation, a full coverage of the nanoparticle is not possible due to steric hindrance, leading to particle growth and consequently, larger particles. The formation of carboxylate bond to the particle's surface occurs with the release of a methane molecule (addition of an absorbed H atom to a CH_3 group of the isopropanol).[33] This step is less favorable than the desorption of a proton in the case of the primary alcohol; therefore, the surface saturation happens over the reaction time leading to an increase of the grafting density throughout the experiment. Moreover, the increased surface coverage can be explained by the grafting of a shorter molecule (due to the release of a CH_4 molecule) leading to a decrease in steric hindrance compared

Table 2 Data on the grafting density and surface coverage for CeO2 NCs synthesized in batch (WL: Weight Loss)

Solvent	Total WL (%)	Corrected WL(%)	Grafting density (molecules.nm^{-2})	Surface coverage (%)
Methanol	*8.12*	*4.16*	*5.09*	*74.4*
Ethanol	*7.49*	*3.55*	*3.23*	*47.2*
Propanol	-	-	-	-
Butanol	*9.40*	*5.05*	*3.14*	*45.9*
Pentanol	-	-	-	-
Hexanol	*9.10*	*4.60*	*1.78*	*26.0*
Isopropanol	*9.54*	*5.29*	*4.20*	*61.4*

to primary alcohol. In our case, the grafting density of isopropanol is between the grafting densities of two primary alcohols: ethanol and propanol. This behavior can be explained by the formation of two different carbon chain lengths of grafted molecules: three carbons when an alkoxide bond (similar to propanol) is formed and only two carbons when a carboxylic bond (similar to ethanol) is formed due to the release of a CH_4 molecule.

The grafting density of CeO_2 NCs synthesized in nc- or sc-alcohol is dependent on the carbon chain length of the alcohol as a result of differences in steric hindrance; and also in the nature of the alcohol (primary or secondary) due to differences in the grafting mechanism (engendering differences in crystallite sizes).

Conclusions

Synthesis of cerium oxide in near- and supercritical alcohols leads to the formation of small nanocrystals (< 10 nm) aggregated into larger nanospheres (100 - 700 nm). Differences measured in crystallite size between batch and continuous mode could be explained by variations in reaction time, oxidation state of cerium precursor and heating rate. As expected, the use of continuous systems allowed a better control of the reaction conditions.

Quantification of grafting density in surface modified CeO_2 nanocrystals synthesized in alcohol was investigated. We suggested here, from the TGA and FTIR results, a direct relationship between the surface coverage of the CeO_2 NCs and the carbon chain length of the alcohol used. Indeed, lower grafting densities were obtained for particles synthesized in longer alcohol chain length. We proposed that the growth step/rate is strongly influenced by the functionalization from the alcohol (solvent). A full surface coverage was almost obtained for material produced in methanol, meaning that all active surface sites are blocked leading to a faster quenching of the growth step. Whereas in longer alcohol chain, steric hindrance prevents a full surface coverage, meaning that the growth of the particle remains possible. Since there is a gradual increase of steric hindrance with alcohol chain length, a continuous increase of nanocrystal size is in agreement with our theory. Thus, these observations explain the correlation between alcohol chain length and the crystallite size in the short residence time continuous experiments. However, this dependence could not be established in the longer batch experiments where desorption of the grafted molecule occurred favouring further growth of the nanocrystals.

Synthesis of cerium oxide synthesis in near- to supercritical alcohols presents a great interest for catalysis (CO_2 capture, exhaust gas cleaning) application thanks to the record surface area measured due to the unique morphology of the nanoparticle assembled into spherical nanostructures. This study demonstrates the possibility to finely control the CeO_2 nanostructures properties, which influences the characteristics but also the thermal behavior and stability of powders.

Acknowledgements

Authors acknowledge the Agence Nationale de la Recherche (contract number: ANR-12-G8ME-0002-01) and the Japan Society for Promotion of Science for financial support in the frame of the G8 Research Councils Initiative on Multilateral Research Fundings: Material Efficiency – A first step towards sustainable manufacturing.

Notes and references

‡ Footnotes relating to the main text should appear here. These might include comments relevant to but not central to the matter under discussion, limited experimental and spectral data, and crystallographic data.

1 J. Zhang, H. Kumagai, K. Yamamura, S. Ohara, S. Takami, A. Morikawa, H. Shinjoh, K. Kaneko, T. Adschiri and A. Suda, Nano Lett., 2011, 11, 361–364.
2 A. Trovarelli, Catal. Rev., 1996, 38, 439–520.
3 C. T. Campbell and C. H. F. Peden, Science, 2005, 309, 713–714.
4 T. Hoshino, Y. Kurata, Y. Terasaki and K. Susa, J. Non-Cryst. Solids, 2001, 283, 129–136.
5 S.-H. Lee, Z. Lu, S. V. Babu and E. Matijević, J. Mater. Res., 2002, 17, 2744–2749.
6 X. Feng, D. C. Sayle, Z. L. Wang, M. S. Paras, B. Santora, A. C. Sutorik, T. X. T. Sayle, Y. Yang, Y. Ding, X. Wang and Y.-S. Her, Science, 2006, 312, 1504–1508.
7 S. Tsunekawa, T. Fukuda and A. Kasuya, J. Appl. Phys., 2000, 87, 1318–1321.
8 R. Li, S. Yabe, M. Yamashita, S. Momose, S. Yoshida, S. Yin and T. Sato, Solid State Ion., 2002, 151, 235–241.
9 S. Yabe and T. Sato, J. Solid State Chem., 2003, 171, 7–11.
10 C. Aymonier, A. Loppinet-Serani, H. Reverón, Y. Garrabos and F. Cansell, J. Supercrit. Fluids, 2006, 38, 242–251.
11 F. Cansell and C. Aymonier, J. Supercrit. Fluids, 2009, 47, 508–516.
12 T. Adschiri, Y.-W. Lee, M. Goto and S. Takami, Green Chem., 2011, 13, 1380–1390.
13 S. K. Pahari, T. Adschiri and A. B. Panda, J. Mater. Chem., 2011, 21, 10377.
14 T. Adschiri, K. Kanazawa and K. Arai, J. Am. Ceram. Soc., 1992, 75, 1019–1022.
15 Y. Hakuta, S. Onai, H. Terayama, T. Adschiri and K. Arai, J. Mater. Sci. Lett., 1998, 17, 1211–1213.
16 T. Adschiri, Y. Hakuta and K. Arai, Ind. Eng. Chem. Res., 2000, 39, 4901–4907.
17 C. Slostowski, S. Marre, J.-M. Bassat and C. Aymonier, J. Supercrit. Fluids, 2013, 84, 89–97.
18 A. Cabanas, J. A. Darr, E. Lester and M. Poliakoff, Chem. Commun., 2000, 901–902.
19 T. Adschiri, Chem. Lett., 2007, 36, 1188–1193.
20 J. Zhang, S. Ohara, M. Umetsu, T. Naka, Y. Hatakeyama and T. Adschiri, Adv. Mater., 2007, 19, 203–206.
21 M. Taguchi, S. Takami, T. Adschiri, T. Nakane, K. Sato and T. Naka, CrystEngComm, 2012, 14, 2132–2138.
22 A. Zenerino, T. Boutard, C. Bignon, S. Amigoni, D. Josse, T. Devers and F. Guittard, Toxicol. Rep., 2015, 2, 1007–1013.

23 A. Pinna, C. Figus, B. Lasio, M. Piccinini, L. Malfatti and P. Innocenzi, ACS Appl. Mater. Interfaces, 2012, 4, 3916–3922.
24 K. Kaneko, K. Inoke, B. Freitag, A. B. Hungria, P. A. Midgley, T. W. Hansen, J. Zhang, S. Ohara and T. Adschiri, Nano Lett., 2007, 7, 421–425.
25 S. S. Lee, W. Song, M. Cho, H. L. Puppala, P. Nguyen, H. Zhu, L. Segatori and V. L. Colvin, ACS Nano, 2013, 7, 9693–9703.
26 A. Fotopoulos, J. Arvanitidis, D. Christofilos, K. Papaggelis, M. Kalyva, K. Triantafyllidis, D. Niarchos, N. Boukos, G. Basina and V. Tzitzios, J. Nanosci. Nanotechnol., 2011, 11, 8593–8598.
27 M. Taguchi, S. Takami, T. Naka and T. Adschiri, Cryst. Growth Des., 2009, 9, 5297–5303.
28 Y. G. Aronoff, B. Chen, G. Lu, C. Seto, J. Schwartz and S. L. Bernasek, J. Am. Chem. Soc., 1997, 119, 259–262.
29 Q. Yuan, H.-H. Duan, L.-L. Li, L.-D. Sun, Y.-W. Zhang and C.-H. Yan, J. Colloid Interface Sci., 2009, 335, 151–167.
30 M. Taguchi, N. Yamamoto, D. Hojo, S. Takami, T. Adschiri, T. Funazukuri and T. Naka, RSC Adv, 2014, 4, 49605–49613.
31 J. Kim, Y.-S. Park, B. Veriansyah, J.-D. Kim and Y.-W. Lee, Chem. Mater., 2008, 20, 6301–6303.
32 B. Veriansyah, H. Park, J.-D. Kim, B. K. Min, Y. H. Shin, Y.-W. Lee and J. Kim, J. Supercrit. Fluids, 2009, 50, 283–291.
33 C. Slostowski, S. Marre, O. Babot, T. Toupance and C. Aymonier, Langmuir, 2012, 28, 16656–16663.
34 C. Slostowski, S. Marre, O. Babot, T. Toupance and C. Aymonier, Langmuir, 2014, 30, 5965–5972.
35 C. Slostowski, S. Marre, O. Babot, T. Toupance and C. Aymonier, *ChemPhysChem*, 2015, DOI: 10.1002/cphc.201500570.
36 M. Taguchi, S. Takami, T. Adschiri, T. Nakane, K. Sato and T. Naka, CrystEngComm, 2011, 13, 2841.
37 G. Cao and Y. Wang, Nanostructures and Nanomaterials: Synthesis, Properties, and Applications, WORLD SCIENTIFIC, 2nd edn., 2011.
38 C. Ho, J. C. Yu, T. Kwong, A. C. Mak and S. Lai, Chem. Mater., 2005, 17, 4514–4522.
39 A. Yee, S. J. Morrison and H. Idriss, J. Catal., 1999, 186, 279–295.
40 H. Idriss, Platin. Met. Rev., 2004, 48, 105–115.

